The American Journal of Human Genetics, Volume *103*

Supplemental Data

MPZL2, Encoding the Epithelial Junctional Protein Myelin Protein Zero-like 2, Is Essential for Hearing in Man and Mouse

Mieke Wesdorp, Silvia Murillo-Cuesta, Theo Peters, Adelaida M. Celaya, Anne Oonk, Margit Schraders, Jaap Oostrik, Elena Gomez-Rosas, Andy J. Beynon, Bas P. Hartel, Kees Okkersen, Hans J.P.M. Koenen, Jack Weeda, Stefan Lelieveld, Nicol C. Voermans, Irma Joosten, Carel B. Hoyng, Peter Lichtner, Henricus P.M. Kunst, Ilse Feenstra, Suzanne E. de Bruijn, DOOFNL Consortium, Ronald J.C. Admiraal, Helger G. Yntema, Erwin van Wijk, Ignacio del Castillo, Pau Serra, Isabel Varela-Nieto, Ronald J.E. Pennings, and Hannie Kremer

Supplemental Figures

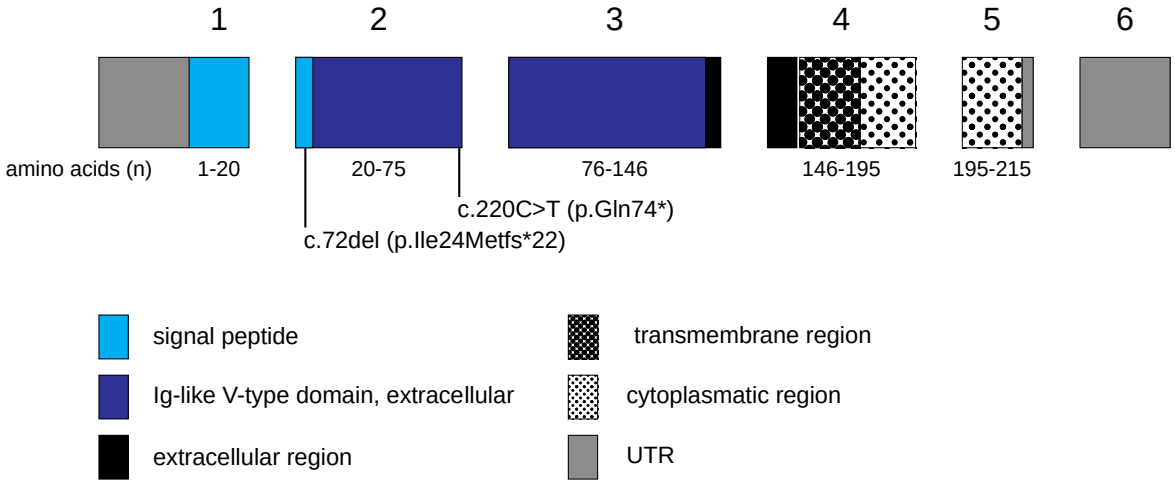

Figure S1. Exonic and protein structure of *MPZL2*/MPZL2 and pathogenic variants
Schematic representation of the genomic structure and the encoded protein domains of *MPZL2* (NM_005797.3). Identified pathogenic variants are indicated. Protein domain predictions were extracted from the SMART domain database (http://smart.embl-heidelberg.de/), using the *PFAM domains* setting.

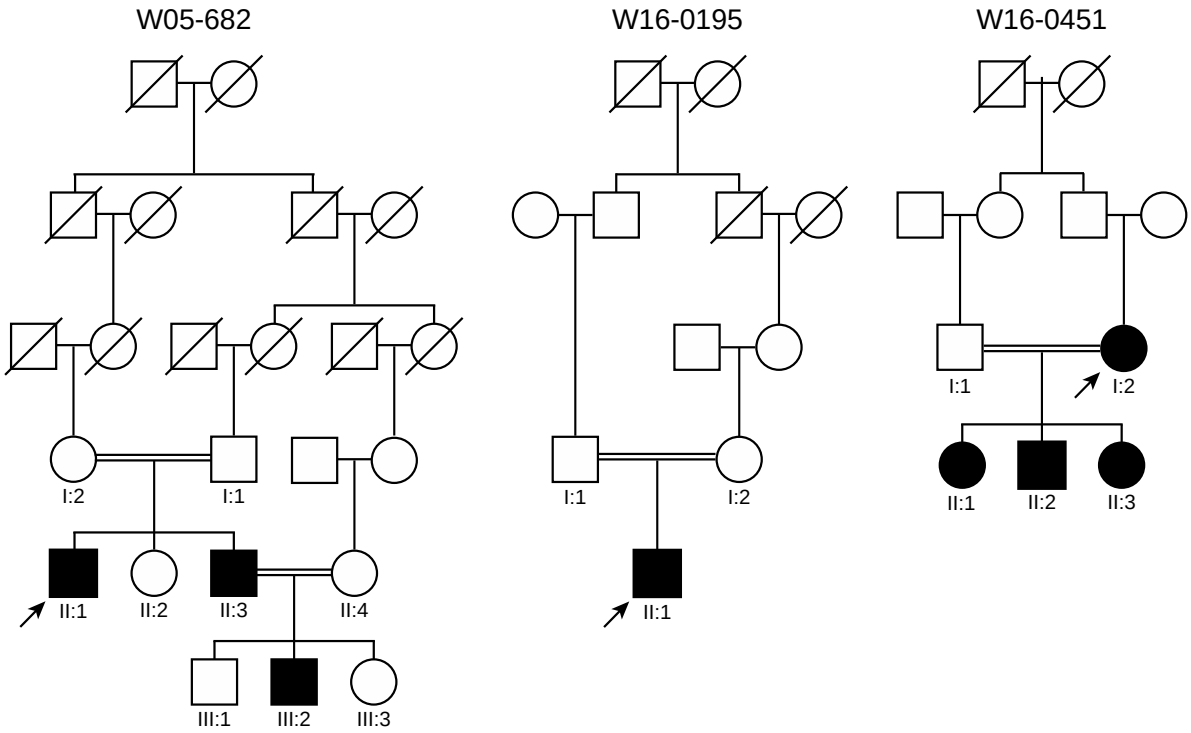

Figure S2. Extended pedigrees of families affected by *MPZL2* variants
Index cases are marked by arrows. Double lines indicate consanguinity.

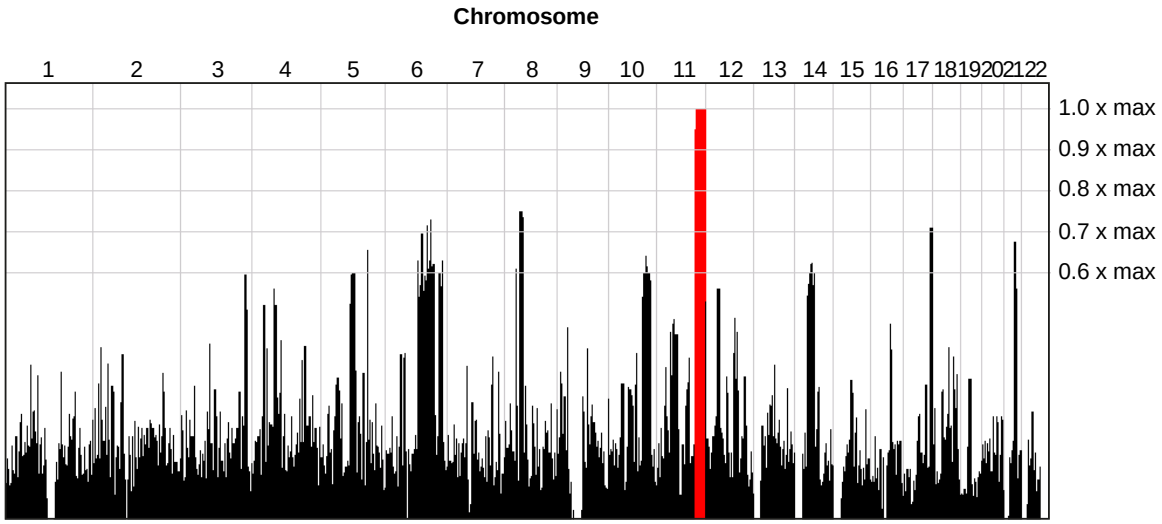

Figure S3. Homozygosity mapping in family W05-682

Graphical representation of the genome-wide homozygosity scores in family W05-682, produced by HomozygosityMapper.[1] Homozygosity mapping was performed by genotyping of subjects II:1 and II:3 of family W05-682 with the Affymetrix mapping 250K SNP array, and subsequent genotype calling with Genotype Console software (Santa Clara, CA, USA) and homozygosity mapping with the online tool HomozygosityMapper (http://www.homozygositymapper.org/). This revealed a single homozygous region of 23.8 Mb on chromosome 11q23.1-q25, flanked by rs4936310 and rs10458997. There were no other significant regions of homozygosity.

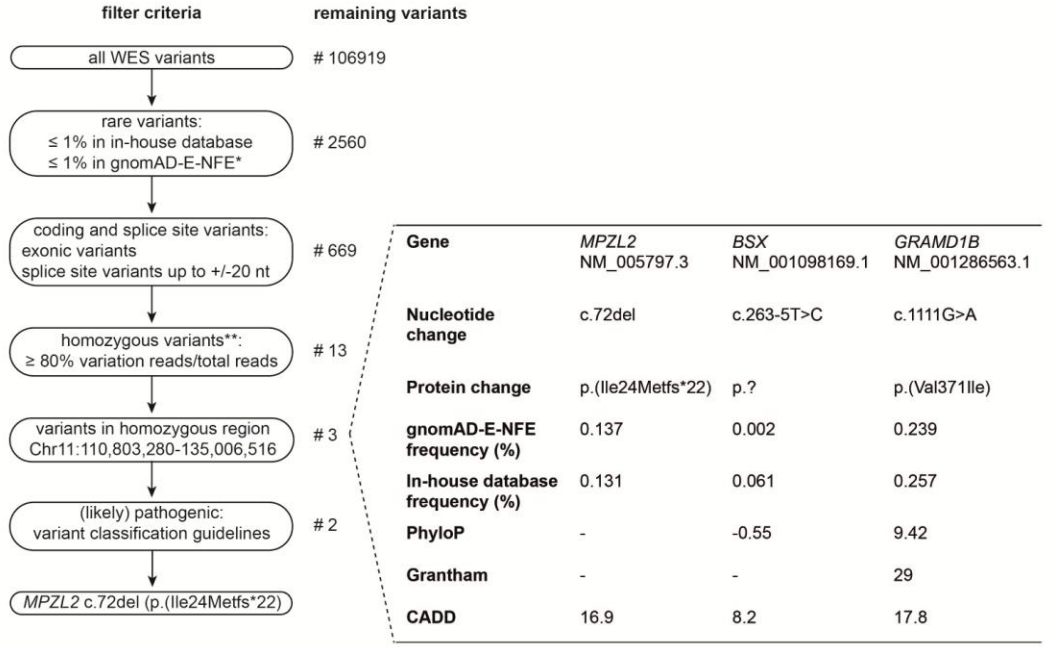

Figure S4. Filtering of WES variants in the largest homozygous region on chromosome 11q23.1-q25 of family W05-682

Criteria of variant filtering and resulting number of variants of WES data for the index case (II:1) of family W05-682. The in-house database contains WES data of ~15,000 individuals, the vast majority of Dutch origin, healthy or affected by different diseases (including 810 subjects with HI). *Minor allele frequencies in the exome data of the the non-Finnish European population in the gnomAD database. **Chromosome X was excluded from the analysis. All 13 homozygous variants are listed in Table S3.

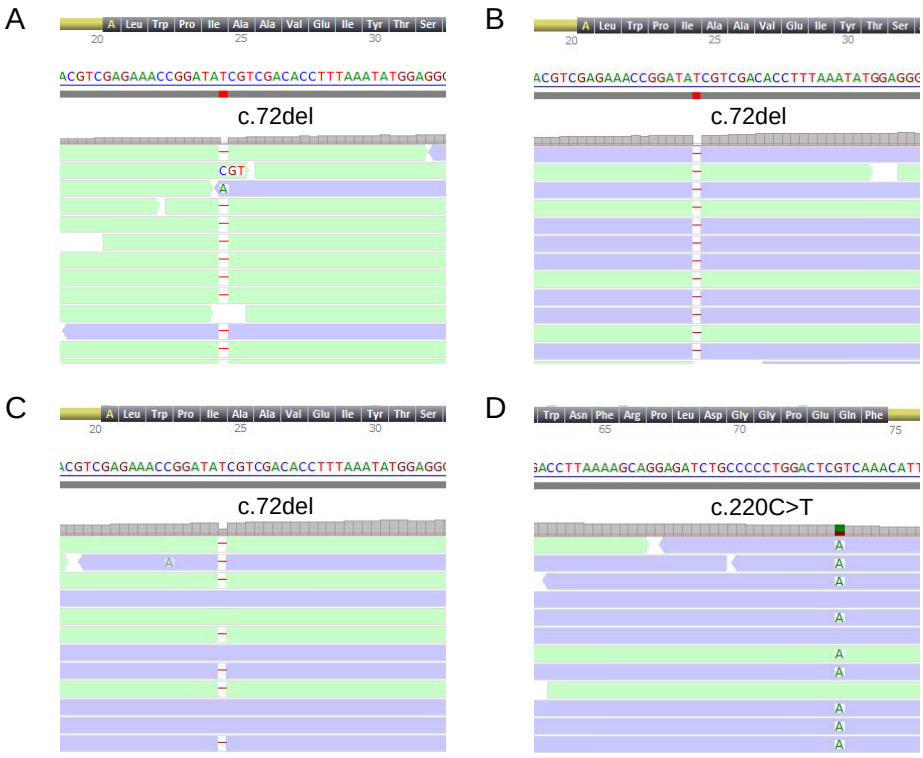

Figure S5. Sequences of *MPZL2* c.72del and c.220C>T

Analysis of the WES paired-reads demonstrated a homozygous point deletion, *MPZL2* c.72del, in the index cases of families W05-682 (**A**) and W16-0195 (**B**). In the index case of family W16-0451, WES revealed the c.72del variant heterozygously (**C**) and the heterozygous missense variant *MPZL2* c.220C>T (**D**). NM_005797.3 was used as reference sequence. Figures were obtained using Alamut Visual (Interactive Biosoftware, Rouen, France).

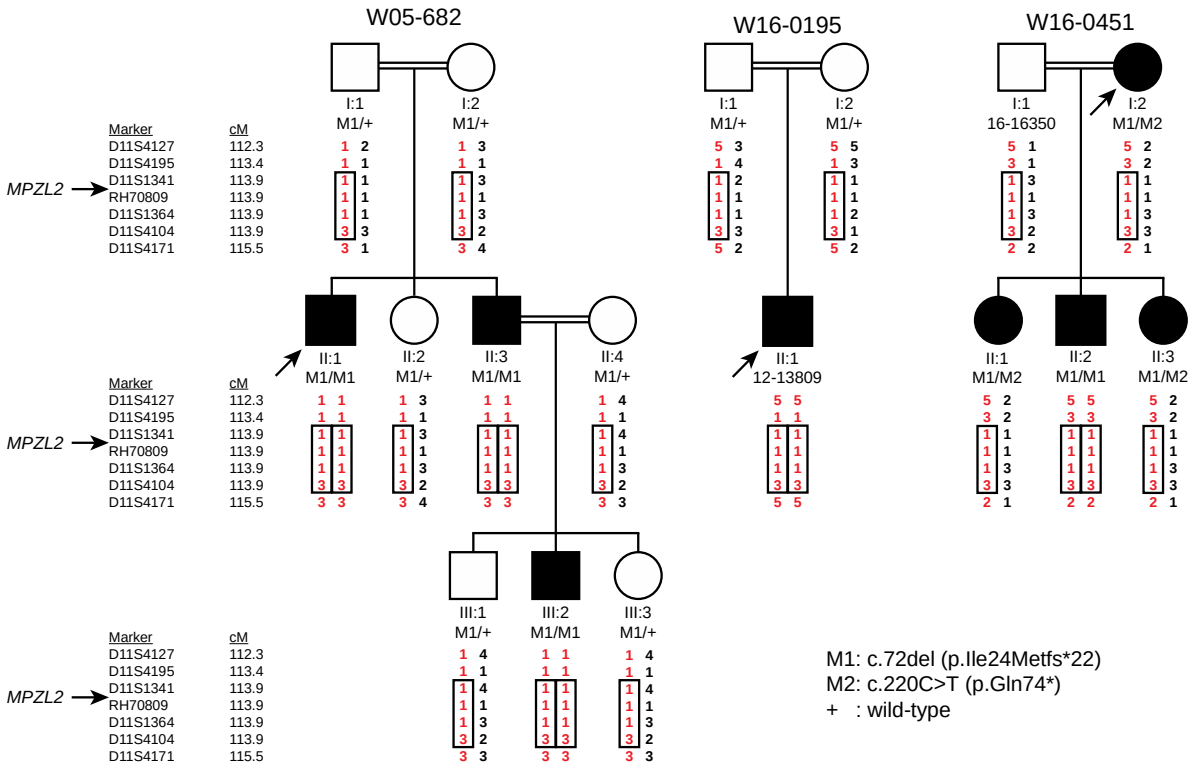

Figure S6. Haplotype analysis of the genomic region harboring *MPZL2*

MPZL2 haplotypes were determined by genotyping VNTR-markers in families W05-682, W16-0195 and W16-0451. All c.72del *MPZL2* alleles (depicted in red) shared a haplotype of at least 0.5 Mb, delimited by markers D11S1341 and D11S4104 (boxed), suggesting that it is derived from a common ancestor. Index cases are marked by arrows.

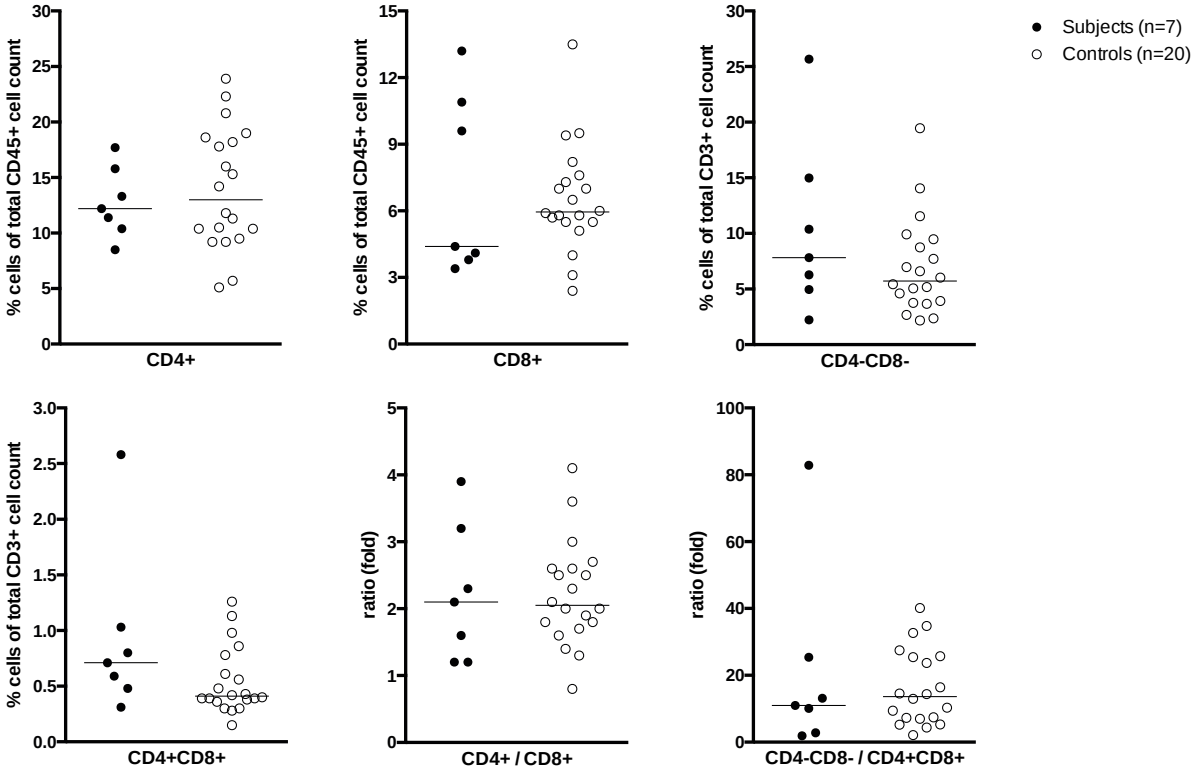

Figure S7. CD4 and CD8 expression on human T cells

The number of CD4 and CD8 expressing human T cells was analyzed in affected individuals (family W05-682, II:1, II:3, III:2; family W16-0195, II:1; family W16-0451, I:2, II:2, II:3), as described in detail before.[4] In brief, peripheral blood was collected in EDTA-tubes, and after red cell lysis, leucocytes were stained with fluorochrome labelled antibodies against CD3 (UCHT-1 pe), CD4 (13B8.2 pacific blue), CD8 (B9.11 APC-AF750) and CD45 (J33 Krome Orange) (all from Beckman Coulter, Brea, USA). Data was acquired on a Navios flow cytometer (Beckman Coulter) and analyzed using Kaluza® software version 1.3 (Beckman Coulter). Presented cell counts are a percentage of total CD45+ cells (CD4+ and CD8+), a percentage of total CD3+ cells (CD4-CD8- and CD4+CD8+) or a fold ratio. Data of 20 healthy individuals was used as control. Individual and median cell counts and ratios are shown. Numbers of cells and ratios are comparable between subjects and controls, indicating normal CD4 and CD8 T cell counts. Mann-Whitney U tests did not demonstrate significant differences.

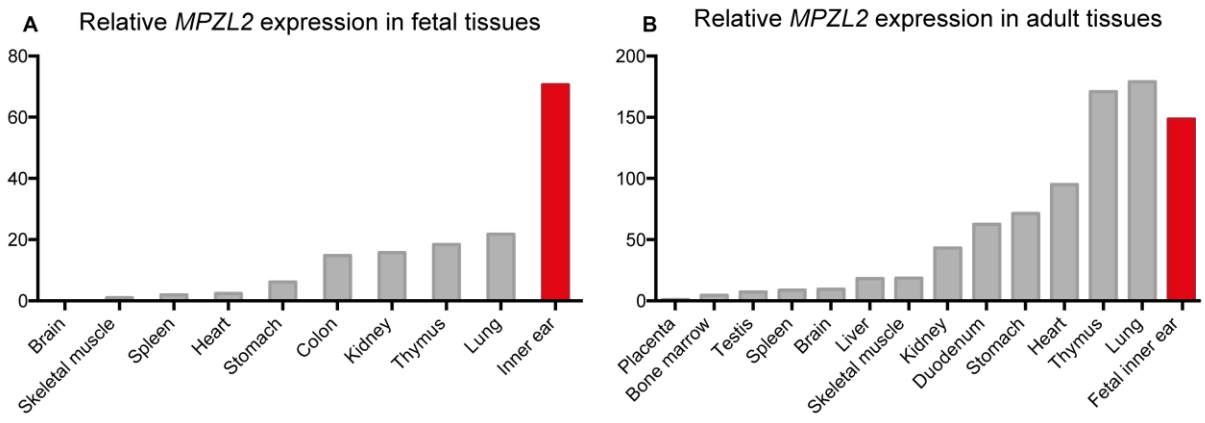

Figure S8. *MPZL2* expression profile in human tissues

Relative *MPZL2* mRNA levels as determined by RT-qPCR in human fetal **(A)** and adult **(B)** tissues. The relative expression values were determined by the delta-delta Ct method with *GUSB* as a reference gene.[2] Expression levels are relative to those in skeletal muscle (**A)** and placenta (**B**), which displayed the lowest detectable *MPZL2* expression of tested fetal and adult tissues, respectively. In fetal brain, no expression of *MPZL2* could be detected. The experiment was performed twice.

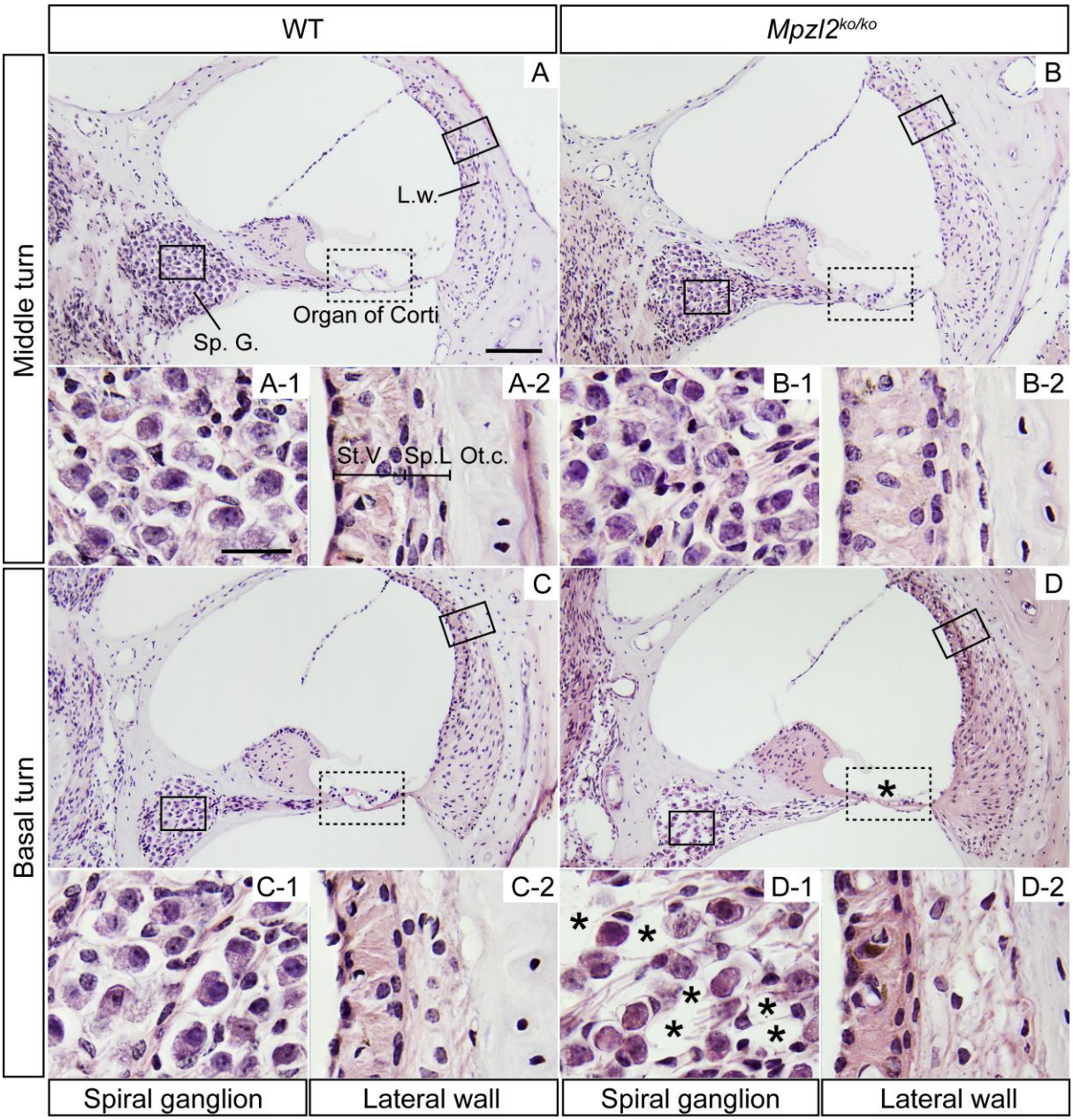

Figure S9. **Cochlear morphology of 12-week-old wild-type mice and *Mpzl2* (*Mpzl2*$^{ko/ko}$) mice**

Representative microphotographs from the middle (**A** and **B**) and basal (**C** and **D**) cochlear turns from midmodiolar cross sections. The second and fourth rows include close-ups of the boxed areas, from left to right: spiral ganglion (1), and stria vascularis (2). Asterisks mark abnormalities. L.w., lateral wall; Ot.c., otic capsule; Sp.G., spiral ganglion; Sp.L., spiral ligament; St.V., stria vascularis. Scale bar A-D, 100 µm, close-ups 25 µm.

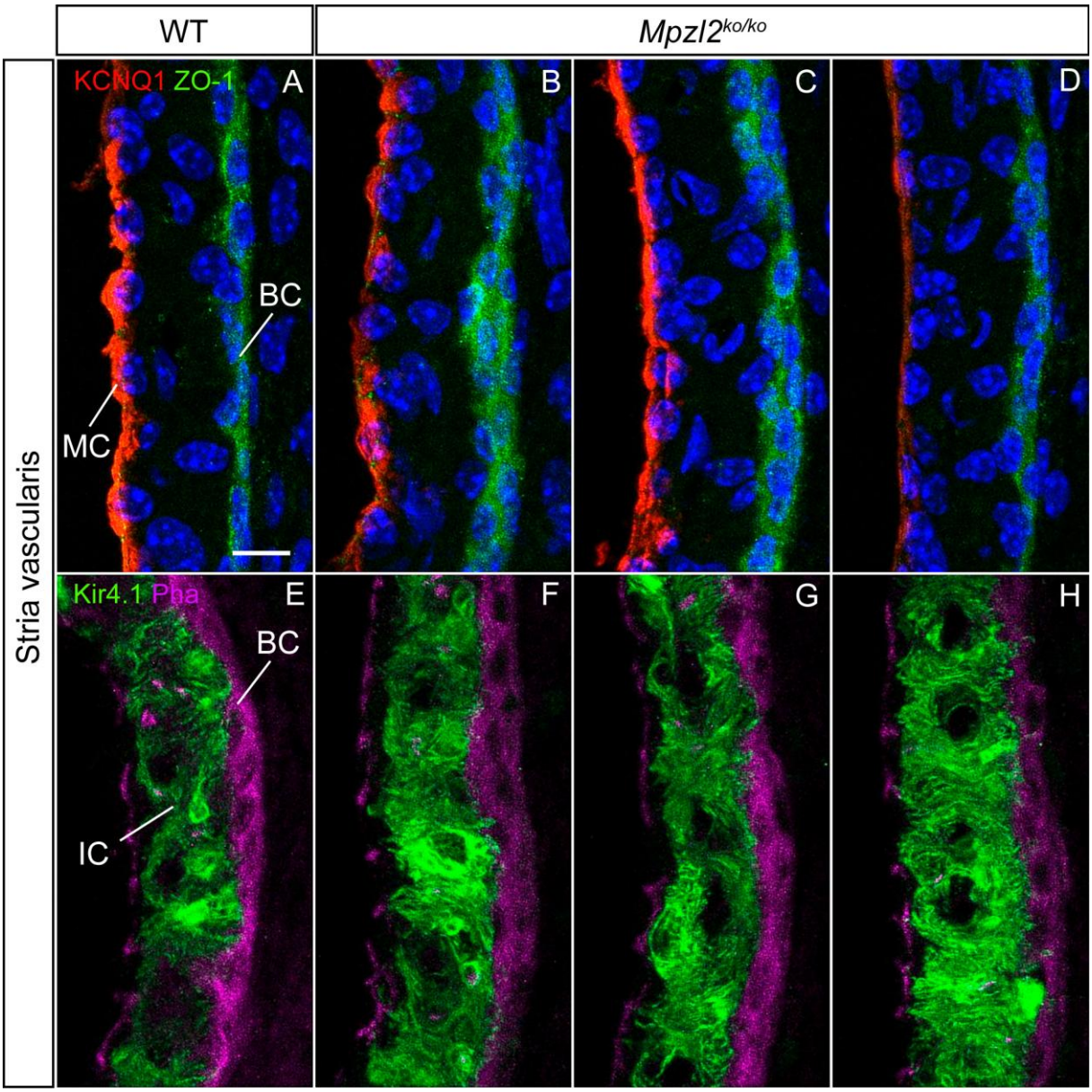

Figure S10. Normal cellular organization of the stria vascularis in wild-type mice and *Mpzl2* (*Mpzl2*$^{ko/ko}$) mice

Close-ups of the stria vascularis (**A-H**) of the basal turn of the cochlea from representative cryosections (10 µm) prepared from a wild-type mouse (**A, E**) and three *Mpzl2* mutant mice (**B-D, F-H**). Strial marginal (MC), basal (BC) and intermediate cells (IC) were immunostained for KCNQ1 (red), ZO-1 (green) (**A-D**) and Kir4.1 (green) (**E-H**) respectively. Actin in the stria vascularis was stained with phalloidin (purple). Scale bar A-H: 10 µm.

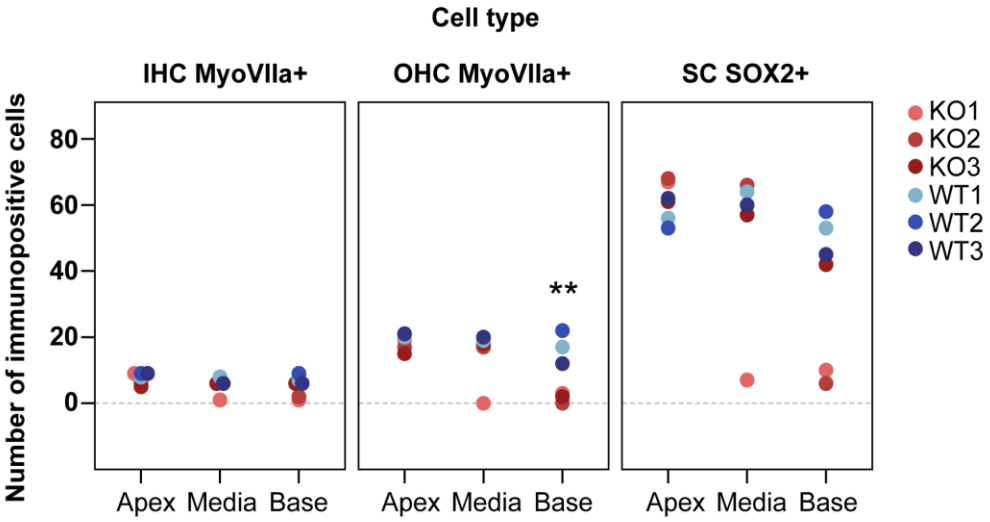

Figure S11. Quantification of MyoVIIa and SOX2 positive cells

Cell numbers were evaluated for wild-type (blue) and Mpzl2 (*Mpzl2*$^{ko/ko}$) mutant mice (red) for each turn of the cochlea. Data were obtained counting MyoVIIa and SOX2 positive cells in each cochlear region from 5 serial cryosections (10 µm) per animal (apex, n=3 mice per genotype in IHC and SC, n=2 wild-type, n= 3 KO in OHC; middle region, n= 2 wild-type, n=3 KO for each cell type; base, n=3 mice per genotype for each cell type). Data are expressed as the sum of each cell type per animal. Cochleae were derived from mice at 12 weeks of age. Statistical analysis was performed by Student t-test between groups for each marker and level of the cochlea. **p<0.01 (KO *versus* WT). IHC, inner hair cells; KO, *Mpzl2* mutant OHC, outer hair cells; SC, supporting cells.

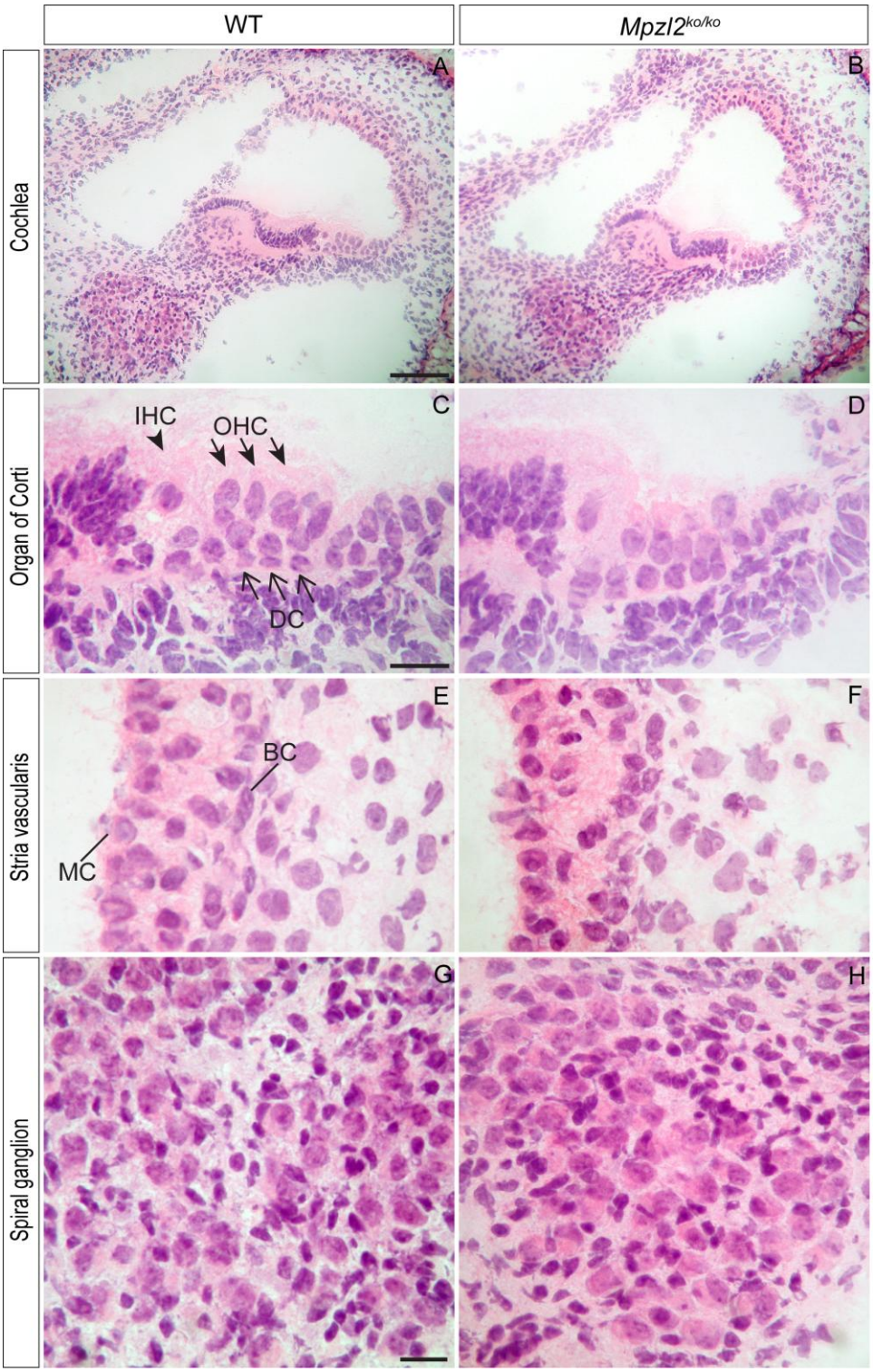

Figure S12. Normal histology of the cochlear basal turn at P4 in wild-type and mutant (*Mpzl2*$^{ko/ko}$) mice

Overview of the basal turn of cochleae (**A, B**) and higher magnifications of organs of Corti (**C, D**), striae vascularis (**E, F**) and spiral ganglions (**G, H**). Arrowheads point to inner hair cells (IHC), blackhead arrows to outer hair cells (OHC) and arrows to Deiters cells (DC). BC, basal cells; MC, marginal cells; WT, wild-type. Scale bars A-B: 100 µm, C-F: 20 µm and G, H: 20 µm.

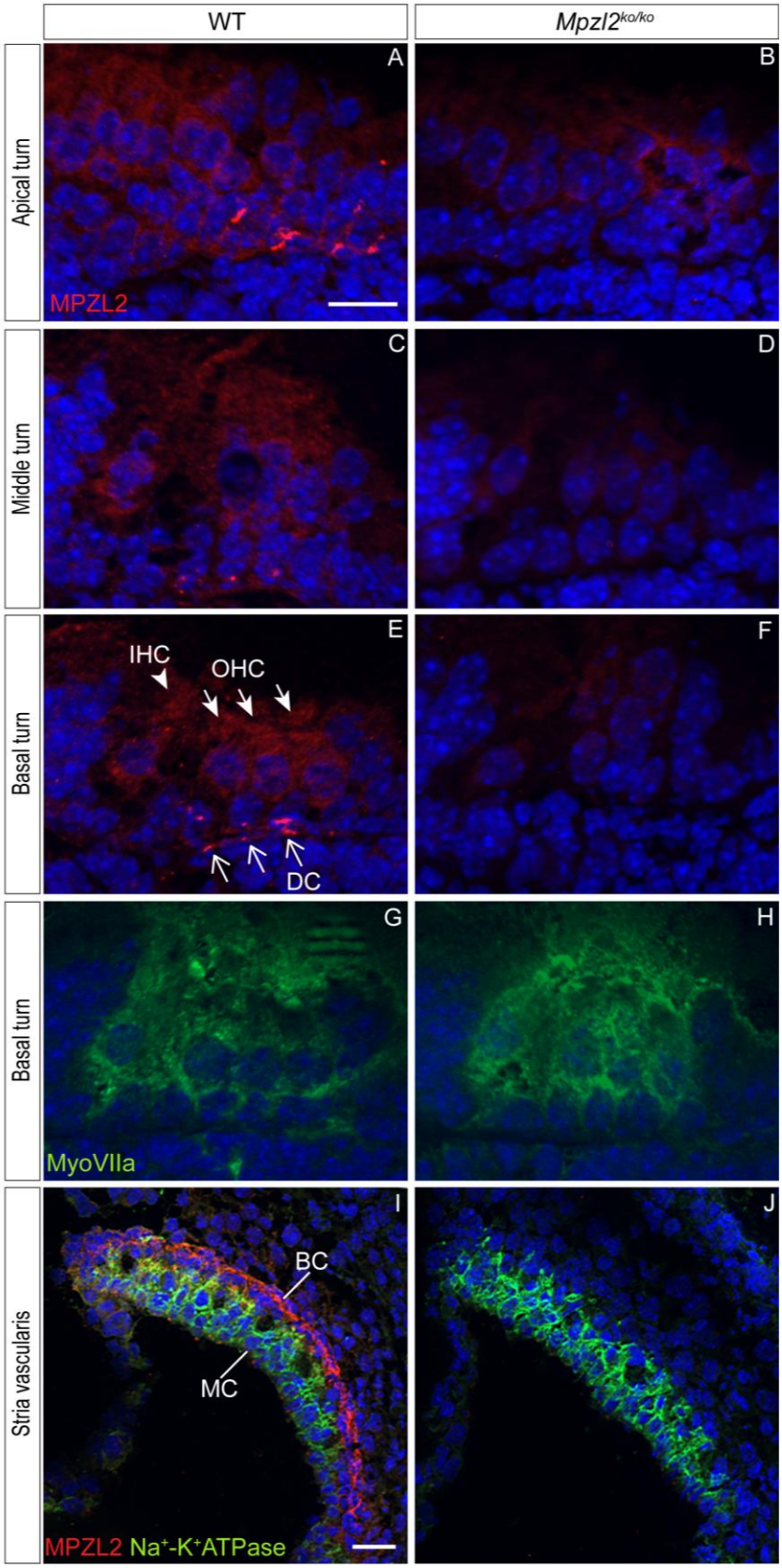

Figure S13. Specificity of immunostaining of MPZL2 in hair cells and Deiters cells of the organ of Corti and basal cells of the stria vascularis in P4 wild-type and Mpzl2 mutant (*Mpzl2*$^{ko/ko}$) mice Immunostaining of MPZL2 (red) is observed diffusely in the hair cells and Deiters cells and with higher intensity at the basal part of the Deiters cells in the

apical (**A**), middle (**C**) and basal (**E**) turns of the cochlea in wild-type mice. Antibody-specificity is confirmed by absence of immunostaining in these cells in the apical (**B**), middle (**D**) and basal (**F**) turns in *Mpzl2* mutant mice. Myosin VIIa (green) immunostaining shows the inner and outer hair cells of the organ of Corti in wild-type (**G**) and *Mpz2* mutants(**H**) mice. In the basal cells of the stria vascularis immunostaining of MPZL2 (red) was observed in the wild-type (**I**) mice and not in *Mpzl2* mutant (**J**) mice. Na^+/K^+-ATPase (green) immunostaining was employed for marking marginal cells (**I, J**). Cell nuclei were stained with DAPI (blue). IHC: inner hair cell, OHC: outer hair cell, DC: Deiters cell, MC: marginal cells, BC: basal cells. Scale bars A-H: 20 µm and I, J: 20 µm.

Supplemental Tables

Table S1. Primer sequences and PCR conditions
For primer design to amplify *MPZL2*, reference sequence NM_005797.3 was used, and for *TECTA*, ENST00000392793.

Table S2. Homozygous regions larger than 1 Mb and WES variants in family W05-682

Start SNP	End SNP	Chr	Start position	End position	Size (Mb)	Known deafness gene(s) in region	WES variants	Rare variants (MAF ≤ 1%)	Coding and splice site variants	(likely) pathogenic variants
rs4936310	rs10458997	11	110,900,760	134,746,130	23.85	*TECTA*	976	22	3	*MPZL2* c.72del
rs9910295	rs7406119	17	76,612,445	81,006,629	4.39	*ACTG1*	480	17	2	-
rs2353200	rs7835152	8	46,924,211	49,623,096	2.70	-	15	3	0	-
rs28870	rs803137	5	129,527,135	132,132,647	2.61	*SLC22A4*	75	1	0	-
rs7125329	rs1648142	11	107,895,836	109,870,952	1.98	-	59	2	0	-
rs10520657	rs12443195	15	88,114,594	90,071,734	1.96	-	62	0	-	-
rs9992997	rs17027362	4	132,958,066	134,644,433	1.69	-	6	0	-	-
rs2236047	rs9472138	6	42,126,399	43,811,762	1.69	-	102	5	0	-
rs4766455	rs12308836	12	109,641,578	111,287,959	1.65	-	42	6	0	-
rs7688203	rs17088085	4	66,568,856	68,057,322	1.49	-	0	0	-	-
rs2451256	rs10755578	6	159,507,338	160,969,738	1.46	-	145	1	0	-
rs1533075	rs9900927	17	63,039,373	64,423,010	1.38	-	37	2	0	-
rs8135828	rs5753355	22	29,929,239	31,259,658	1.33	-	66	2	0	-
rs7152200	rs8022938	14	66,836,155	67,855,327	1.02	-	7	1	0	-
rs7574269	rs6735340	2	14,700,457	15,705,915	1.01	-	59	1	0	-

Homozygous regions of shared genotypes. Genomic positions were determined using the UCSC Genome Browser, GRCh37/hg19 (https://genome.ucsc.edu/). The intronic variant of SLC22A4 (MIM: 604190; DFNB60) is not predicted to affect splicing. Coding and splice site base pairs of known deafness genes were covered by the indicated number of reads: TECTA ≥15; ACTG1 ≥15; SLC22A4 ≥20.

Table S3. Rare homozygous WES variants in family W05-682

Chr	Position	Ref	Var	AF_in house	Gnom AD_E AF NFE	Gene	Transcript	cDNA	Protein	CADD_ PHRED	SIFT	PPH2	Mutation Taster
chr6	90383869	C	T	0.28	0.43	*MDN1*	NM_014611.2	c.13201G>A	p.Val4401Ile	2.38	0.00	0.002	Disease causing
chr6	99729213	T	C	0.18	0.13	*FAXC*	NM_032511.3	c.1057A>G	p.Lys353Glu	13.22	0.05	0.040	Disease causing
chr6	116943955	G	A	0.02	0.00	*RSPH4A*	NM_001010892.2	c.711G>A	p.=	8.44	-	-	-
chr8	8176387	C	G	0.32	-	*SGK223*	NM_001080826.2	c.3498G>C	p.=	0.02	-	-	-
chr11	640090	G	C	0.98	-	*DRD4*	NM_000797.3	c.841G>C	p.Ala281Pro	9.47	1.00	0.000	Polymorphism
chr11	**118133799**	**T**		**0.13**	**0.14**	***MPZL2***	**NM_005797.3**	**c.72del**	**p.Ile24Metfs***	16.91	-	-	-
chr11	**122850170**	**A**	**G**	**0.06**	**0.00**	***BSX***	**NM_001098169.1**	**c.263-5T>C**	**p.?**	8.18	-	-	-
chr11	**123479372**	**G**	**A**	**0.26**	**0.24**	***GRAMD1B***	**NM_001286563.1**	**c.1111G>A**	**p.Val371Ile**	17.82	0.09	0.206	Disease causing
chr17	39340843	G	A	0.17	0.29	*KRTAP4-1*	NM_033060.2	c.264C>T	p.=	4.66	-	-	-
chr17	39340852	G	A	0.10	0.30	*KRTAP4-1*	NM_033060.2	c.255C>T	p.=	8.95	-	-	-
chr17	79082774	C	T	0.16	0.25	*BAIAP2*	NM_017450.2	c.1542C>T	p.=	9.92	-	-	-
chr17	80395141	T	C	0.04	0.00	*HEXDC*	NM_173620.2	c.801T>C	p.=	0.45	-	-	-
chr19	53117017	T	G	-	-	*ZNF83*	NM_001105549.1	c.801A>C	p.=	0.04	-	-	-

Variants indicated in bold are in the shared 23.85 Mb homozygous region of chromosome 11 and co-segregated with the HI in the family. Variants of *MDN1* and *FAXC* did not segregate with the disease. For none of the variants an effect on transcript splicing was predicted and none of the variants was present in the ClinVar database. Genomic positions are according to GRCh37/hg19. AF_inhouse (%) represent allele frequencies in the in-house database of ~15,000 exomes. Gnom AD_E AF NFE, allele frequency (%) in GnomAD, exomes of non-Finnish Europeans; PPH2, PolyPhen-2. Scores that meet the thresholds for pathogenicity as indicated in ‘Subjects and Methods’ are indicated in red.

Table S4. WES variants of *TECTA* in family W05-682

Chr	Position	Ref	Var	AF_in house	Gnom AD_E AF NFE	Gnom AD_G AF NFE	cDNA	Protein	PhyloP	CADD_ PHRED	SIFT	MutationTaster	PPH2	ClinVar
chr11	120976413	G	A	39.67	-	39.47	c.65-127G>A	p.?	0.872	8.62	-	-	-	-
chr11	120976428	A	G	49.35	-	48.75	c.65-112A>G	p.?	-2.755	0.89	-	-	-	-
chr11	120984087	C	G	23.51	-	26.46	c.624+169C>G	p.?	-1.978	0.41	-	-	-	-
chr11	120989335	A	G	39.81	41.30	42.88	c.1111A>G	p.Arg371Gly	4.856	3.89	1.00	Polymorphism	0.000	UV1
chr11	121007948	C	T	18.69	-	-1.00	c.2942-182C>T	p.?	-1.365	0.21	-	-	-	-
chr11	121016098	T	C	19.33	-	20.93	c.3544-166T>C	p.?	0.401	15.71	-	-	-	-
chr11	121016145	G	A	20.10	-	20.92	c.3544-119G>A	p.?	-0.469	7.34	-	-	-	-
chr11	121016818	G	A	20.14	21.15	20.95	c.4098G>A	p.=	-3.629	3.59	-	-	-	UV1
chr11	121016838	C	T	19.32	20.75	20.48	c.4105+13C>T	p.?	0.784	3.22	-	-	-	UV1
chr11	121023992	A	G	14.95	-	33.67	c.4305+203A>G	p.?	-0.213	8.36	-	-	-	-
chr11	121033105	A	G	35.76	34.46	33.76	c.5272+26A>G	p.?	0.172	8.76	-	-	-	-
chr11	121033277	C	T	18.95	-	33.65	c.5272+198C>T	p.?	-0.867	6.61	-	-	-	-
chr11	121035860	G	T	33.99	-	33.63	c.5273-122G>T	p.?	-0.110	6.56	-	-	-	-
chr11	121037530	G	A	20.14	20.91	20.70	c.5586+41G>A	p.?	1.650	11.75	-	-	-	-
chr11	121037554	T	C	20.03	-	20.67	c.5586+65T>C	p.?	0.044	7.73	-	-	-	-
chr11	121039234	T	C	18.35	-	20.63	c.5751-152T>C	p.?	0.251	8.22	-	-	-	-

For none of the variants an effect on transcript splicing is predicted. Genomic positions are according to GRCh37/hg19. AF_inhouse (%) represent allele frequencies in the in-house database of ~15,000 exomes; Gnom AD_E AF NFE, allele frequency (%) in Gnom AD, exomes of non-Finnish Europeans; Gnom AD_G AF NFE, allele frequency (%) in Gnom AD, genomes of non-Finnish Europeans; PPH2, PolyPhen-2. PhyloP represents the phyloP100way score. Effect on cDNA is based on transcript NM_005422.2.

Table S5. Analysis of intragenic deletions in subjects with a heterozygous variant in *MPZL2*

Sample	Identified heterozygous variant	Gender	Mean Ct value *MPZL2* exon 2	Mean Ct value *MPZL2* exon 3	Mean Ct value *MPZL2* exon 5	Mean Ct value *SLC16A2* exon 6
DNA11-22171	c.544C>T (p.(Arg182*)), exon 4	female	25	24	25	24
DNA11-23140	c.268C>T (p.(Arg90Trp)), exon 3	male	25	24	25	25
Control		female	25	24	25	24

In two individuals of the phenotype-based cohort, rare mono-allelic variants of *MPZL2* were identified. As no variants could be detected of the second allele by Sanger sequencing, genomic qPCR was performed to identify possible intragenic deletions. qPCR was performed for exons without a heterozygous SNP (*MPZL2* exons 2, 3 and 5). Temperatures and reaction times for qPCR were as follows: 10 min at 95 °C, followed by 40 cycles of 15 sec at 95 °C and 30 sec at 60 °C. qPCRs were performed with the Applied Biosystem Fast 7900 System in accordance with the manufacturer's protocol (Applied Biosystems, Foster City, CA, USA). *SLC16A2* (MIM: 300095) was employed as a reference gene. All reactions were performed in duplicate, mean Ct values are indicated. These Ct values do not provide any indication for the presence of intragenic deletions encompassing exons 2, 3, or 5 of *MPZL2.*

Table S6. Shared rare homozygous and compound heterozygous WES variants in family W16-0451

Chr	Position	Ref	Var	AF_in house	Gnom AD_E AF	Gnom AD_G AF	Gene	Transcript	cDNA variant	Protein variant	CADD_ PHRED	SIFT	PPH2	MutationTaster
								Homozygous						
chr1	14105151	TGA		0.60	-	0.34	*PRDM2*	NM_012231.4	c.861_863del	p.Asp287del	12.41	-	-	-
chr16	69988459	T	G	0.19	0.03	0.01	*CLEC18A*	NM_182619.3	c.439T>G	p.Cys147Gly	15.91	0.02	0.357	Disease causing
								Compound heterozygous						
chr1	228404296	C	T	0.00	-	0.01	*OBSCN*	NM_001271223.2	c.2270C>T	p.Ser757Leu	4.84	0.01	0.005	Polymorphism
chr1	228526578	T	A	0.83	0.81	0.84	*OBSCN*	NM_001271223.2	c.19980T>A	p.Ser6660Arg	18.55	0.00	0.690	Polymorphism
chr6	168315860	A	G	0.00	-	0.00	*AFDN*	NM_001291964.1	c.2168A>G	p.His723Arg	14.37	0.00	0.273	Disease causing
chr6	168317830	C	G	0.00	0.00	0.00	*AFDN*	NM_001291964.1	c.2483C>G	p.Thr828Ser	26.10	0.02	0.803	Disease causing
chr11	118133799	T	-	0.13	0.08	0.04	*MPZL2*	NM_005797.3	c.72del	p.Ile24Metfs*	16.91	-	-	-
chr11	118133651	G	A	0.02	0.04	0.04	*MPZL2*	NM_005797.3	c.220C>T	p.Gln74*	39	-	-	-
chr14	104433097	A	G	0.20	0.27	0.43	*TDRD9*	NM_153046.2	c.694A>G	p.Thr232Ala	16.61	0.00	0.558	Disease causing
chr14	104497541	C	T	0.00	0.00	-	*TDRD9*	NM_153046.2	c.3379C>T	p.Leu1127Phe	9.49	0.07	0.698	Polymorphism
chr22	26173565	C	T	0.00	0.01	0.03	*MYO18B*	NM_001318245.1	c.1885C>T	p.Arg629Trp	13.02	0.01	0.007	Polymorphism
chr22	26422656	C	G	0.02	0.02	0.02	*MYO18B*	NM_001318245.1	c.6719C>G	p.Ser2240Trp	18.35	0.00	0.878	Polymorphism

Genomic positions are according to GRCh37/hg19. For none of the variants an effect on transcript splicing is predicted and none of the variants is present in ClinVar**.** AF_inhouse is indicated in %. Gnom AD_E AF, allele frequency (%) in Gnom AD, exomes; Gnom AD_G AF, allele frequency (%) in Gnom AD, genomes; PPH2, PolyPhen-2. Scores that meet the thresholds for pathogenicity are indicated in red. Only the homozygous variant of *PRDM2* co-segregated with the disease.

Table S7. Individual results of otoscopy, tympanometry, pure-tone audiometry, OAEs, acoustic reflexes, HI progression and speech discrimination

Family	Subject	Age at evaluation (years)	Reported onset age of HI (years)	Otoscopic examination	Tympano-metry	PTA (dB HL)	OAEs	Mean ART	Statistically significant progression of HI (follow-up)	SRT (dB)	Maximum SRS (%)
W05-682	II:1	37	4	normal	R+L type A	60	R+L ND	100 dB	yes (21 years)	50	100
	II:3	42	9	R+L myringo-sclerosis	R+L type A	65	R+L ND	100 dB	yes (20 years)	53	100
	III:2	9	4	normal	R+L type A	37	R+L ND	90 dB	no (4 years)	32	90
W16-0195	II:1	8	3	normal	R type A L type Ad	40	R+L ND	90 dB	no (3 years)	30	100
W16-0451	I:2	44	childhood	normal	R+L type A	48	R+L ND	90 dB	yes (10 years)	31	92
	II:1	13	3	NT	NT	35	NT	NT	no (7 years)	NT	NT
	II:2	16	5	normal	R+L type A	38	R ND L detected at 1 kHz	90 dB	no (5 years)	27	95
	II:3	7	6	normal	R+L type A	35	R+L detected at 1.4kHz	90 dB	no (1 year)	28	95

PTA, pure tone average, mean thresholds of 0.5, 1 and 2 kHz in dB HL; OAEs, otoacoustic emissions; ART, acoustic reflex threshold; SRT, speech reception threshold; SRS, speech recognition score; R, right; L, left; ND, not detected; NT, not tested. Tympanometry type A means a normal curve, indicating normal pressure in the middle ear with normal mobility of the eardrum and ossicles; type Ad means a higher curve, indicating increased mobility of the eardrum and/or ossicles. Progression of HI was considered significant if at least 2 frequencies showed significant progression ($p \leq 0.05$). Results of audiometry, acoustic reflexes and speech discrimination from the better hearing ear are presented. One of the siblings (II:1) of family W16-0451 was not able to participate in the clinical evaluation; only retrospective data of this subject were used for analysis.

Table S8. Individual results of ABR and vestibular tests

Family	Subject	Click-evoked ABR	History of vestibular symptoms	Rotary chair test	Caloric irrigation test	vHIT	cVEMP
W05-682	II:1	symmetric, normal wave latencies	no	normal	normal	normal	normal (slightly lower)
	II:3	NT	no	NT	NT	NT	NT
	III:2	NT	no	NT	NT	NT	NT
W16-0195	II:1	symmetric, normal wave latencies	no	NT	NT	NT	NT
W16-0451	I:2	NT	two periods of vertigo in the past, without persisting complaints	normal	normal	normal	normal (slightly lower)
	II:1	NT	unknown	NT	NT	NT	NT
	II:2	NT	no	normal	slight asymmetry to the detriment of the left vestibulum	normal	normal (slightly lower)
	II:3	NT	no	NT	NT	NT	NT

ABR, auditory brainstem response; vHIT, video head impulse test; cVEMP, cervical vestibular evoked myogenic potentials; NT, not tested.

Supplemental Methods

Screening protocol for polyneuropathy in subjects with *MPZL2* variants

Medical history was obtained regarding sensory disturbances, muscle weakness, functional impairment (walking, walking stairs, cycling), and use of medication. Participants also underwent physical neurological examination.

Neurological examination included testing of:

- Cranial nerves, according to current standards
- Muscle strength using the Medical Research Council (MRC) scores (0-5) of 18 predefined muscle groups, including shoulder abduction, elbow flexion, wrist extension, hip flexion, knee extension, foot dorsiflexion (extension) and plantar flexion, and toe dorsiflexon (extension); muscle tone and bulk
- Muscle mass of the extensor digitorum brevis muscle (normal / atrophic)
- Vigorimeter grip strength, as described previously[3]
- Coordination with use of nose-finger test and tandem gait (normal / abnormal).
- Sensation, using the Modified INCAT Sensory Sum Score (mISSReflexes) and the Romberg test (1= abnormal; 0 = normal), according to the European Federation of Neurological Societies/Peripheral Nerve Society guideline on management of chronic inflammatory demyelinating polyradiculoneuropathy[4]
- Deep tendon reflexes (biceps, triceps, patellar and ankle jerks) bilaterally (absent / reduced / normal)

Screening for immunological defects and defects of the cornea and vision

Immunological screening was performed to evaluate presence of immunodeficiencies by asking participants about symptoms of allergies, autoimmune diseases, and frequent, prolonged or severe infections or inflammations. In addition, the numbers of CD4- and CD8-expressing human T cells were analyzed, using flow cytometry, as indicated in the legend of Figure S7. Screening for corneal abnormalities and vision problems was performed by history, slit lamp biomicroscopy and evaluation of visual acuity using a Snellen chart.

In silico evaluation of missense variants and prediction of effects on splicing

Prediction of a potential pathogenic effect of missense variants was performed with CADD PHRED[5] (≥15), SIFT (≤0.05), PolyPhen-2 (PPH2, ≥0.450) and Mutation Taster[6] (deleterious). Values for predicted pathogenicity are indicated between brackets. Segregation analysis was performed if at least two of the tools predicted a pathogenic effect of the variant. In case of more than one rare heterozygous variant in a gene, segregation analysis was performed if the pathogenicity criteria were met for one of the variants. A potential effect on splicing was predicted with the tools SpliceSiteFinder-like, MaxEntScan, NNSPLICE, GeneSplicer, and Human Splicing Finder as available in Alamut Visual (version 2.10, Interactive Biosoftware, Rouen, France). A change of at least 30% of splice site scores in at least two of the tools was regarded significant. Also PPH2 and SIFT were employed via Alamut Visual.

Quantitative PCR (qPCR) analysis for identification of intragenic deletions

We quantified copy numbers of *MPZL2* exons 2, 3 and 5 by using genomic qPCR. Specific primers (Table S1) were designed with Primer3Plus and reference sequence NM_005797.3. qPCRs were performed with 5 *μ*g genomic DNA and reaction mixtures were prepared with the GoTaq qPCR Master Mix (Promega) in accordance with the manufacturer's protocol. qPCRs were performed with the Applied Biosystem Fast 7900 System in accordance with the manufacturer's protocol (Applied Biosystems). *SLC16A2* (MIM: 300095) was employed as a reference gene. All reactions were performed in duplicate.

Histology and immunohistochemistry of cochleae from wild-type and *Mpzl2* mutant mice

Cochleae from 12 weeks old mice (n=3 per genotype) were dissected, decalcified and embedded in paraffin or Tissue-Tek OCT (Sakura Finetek). Deparaffinized cochlear sections (5 μm) were stained with hematoxylin and eosin, and images for general cytoarchitecture evaluation were taken with 10x, 20x and 40x magnification objectives with an Olympus DP70 digital camera as described previously.[7] For immunofluorescence assays of 12-week cochleae, cryosections (10 μm) were treated overnight at 4ºC with the following primary antibodies: rabbit anti-Kir4.1 (1:200 AB5818 Chemicon), rat anti-ZO-1 (1:200 sc-33725 Santa Cruz); rabbit anti-KCNQ1 (1:200 sc-20816 Santa Cruz), rabbit anti-Myosin VIIa (1:250 25-6790 Proteus), or goat anti-SOX2 (1:100 sc-17320 SantaCruz). After washing, sections were incubated with the corresponding secondary Alexa conjugated antibodies for 2 hrs at room temperature (RT), essentially as reported in Sanchez-Calderon *et al.* (2010).[8]

Images were taken with epifluorescence (Nikon 90i, Tokyo, Japan) and/or confocal (Leica TCS SP2; Leica, Wetzlar, Germany) microscopes. SOX2 and Myosin VIIa positive cells were counted from base to apex in five serial cryosections (10 μm) per animal separated by 50 μm, prepared from 3 mice of each genotype. The intensities of KCNQ1, ZO-1, and Kir4.1 immunostainings were determined in areas of the stria vascularis, delimited by thresholding the marker's fluorescent signal using Fiji software v1.51n (National Institutes of Health, Bethesda, MD, USA). The fluorescence optical density was thus determined from base to apex in 3-5 serial cryosections (10 μm) per animal separated by 50 μm, prepared from 3 mice of each genotype. Statistical significance was determined by Student's t test for unpaired samples.

For evaluation of early postnatal cytoarchitecture of the cochlea and for localization of MPZL2, inner ears of postnatal day four (P4) C57BL6J wild-type and *Mpzl2* mutant mice (n=3) were dissected, cryoprotected with 10% sucrose in PBS before embedding in Tissue-Tek OCT. For analysis of the cytoarchitecture, cryosections (7 μm) were fixed with paraformaldehyde (PFA) 4% (10 min), stained with hematoxylin and eosin, and analyzed on a Zeiss Axioskop light microscope. For immunofluorescence, cryosections were permeabilised with 0.01% Tween20 in PBS (20 min) and after rinsing with PBS and blocking with blocking buffer (ovalbumin 0.1% and fish gelatin 0.5% in PBS; 1 hr) incubated overnight at 4 ºC with primary antibodies diluted in blocking buffer. After rinsing with PBS, cryosections were incubated (1 hr) with secondary antibodies diluted in blocking buffer with DAPI (1:8000; D1306; Molecular Probes). After rinsing in PBS, sections were fixed in PFA 4% in PBS (10 min), rinsed and mounted in anti-fade Prolong Gold (P36930; Molecular Probes). Analyses were performed on a Zeiss Axio Imager fluorescence microscope and for higher resolution on a Zeiss LSM880 confocal microscope. As primary antibodies were used: Rabbit anti-MPZL2, raised against the complete protein (1:200 11787-1-AP Proteintech,), rabbit anti-

Myosin VIIa (1:200 25-6790 Proteus), goat anti-Collagen IV (1:200 1340-01 SouthernBiotech), and mouse anti-Na^+-K^+ATPase α1 (1:5 α6F Developmental Studies Hybridoma Bank). As secondary antibodies were utilized: Alexa Fluor (AF) conjugated immunoglobulins (Molecular Probes): AF 568-goat anti-rabbit (A11011), AF 488-donkey anti-goat (A11055), AF 488-goat anti-mouse (A11029) and AF 488-goat anti-rat (A11006), at a 1:800 dilution.

Supplemental References

1. Seelow D, Schuelke M, Hildebrandt F, Nurnberg P. HomozygosityMapper--an interactive approach to homozygosity mapping. *Nucleic Acids Research.* 2009;37(Web Server issue):W593-599.
2. Pfaffl MW. A new mathematical model for relative quantification in real-time RT-PCR. *Nucleic Acids Research.* 2001;29(9):e45.
3. Vanhoutte EK, Latov N, Deng C, et al. Vigorimeter grip strength in CIDP: a responsive tool that rapidly measures the effect of IVIG--the ICE study. *European Journal of Neurology.* 2013;20(5):748-755.
4. Van den Bergh PY, Hadden RD, Bouche P, et al. European Federation of Neurological Societies/Peripheral Nerve Society guideline on management of chronic inflammatory demyelinating polyradiculoneuropathy: report of a joint task force of the European Federation of Neurological Societies and the Peripheral Nerve Society - first revision. *European Journal of Neurology.* 2010;17(3):356-363.
5. Kircher M, Witten DM, Jain P, O'Roak BJ, Cooper GM, Shendure J. A general framework for estimating the relative pathogenicity of human genetic variants. *Nature Genetics.* 2014;46(3):310-+.
6. Schwarz JM, Cooper DN, Schuelke M, Seelow D. MutationTaster2: mutation prediction for the deep-sequencing age. *Nature Methods.* 2014;11(4):361-362.
7. Martinez-Vega R, Garrido F, Partearroyo T, et al. Folic acid deficiency induces premature hearing loss through mechanisms involving cochlear oxidative stress and impairment of homocysteine metabolism. *FASEB Journal.* 2015;29(2):418-432.
8. Sanchez-Calderon H, Rodriguez-de la Rosa L, Milo M, Pichel JG, Holley M, Varela-Nieto I. RNA microarray analysis in prenatal mouse cochlea reveals novel IGF-I target genes: implication of MEF2 and FOXM1 transcription factors. *PLoS One.* 2010;5(1):e8699.